Super-light sterile neutrinos at Borexino and KamLAND

Zikang Chen Jiajun Liao Jiajie Ling Baobiao Yue

School of Physics, Sun Yat-sen University

Abstract

The presence of a super-light sterile neutrino can lead to a dip in the survival probability of solar neutrinos, and explain the suppression of the upturn in the low energy solar neutrino data. In this work, we perform a systematical study of the propagation of solar neutrinos in the presence of a super-light sterile neutrino by taking into account of the non-adiabatic transitions and the coherence effect. In particular, we obtain an analytic equation that can predict the position of the dip. We also place constraints on the sterile neutrino parameter space in the 3+1 framework using the current Borexino and KamLAND data.

Motivation

Current measurements of the smallest mass splitting among active neutrinos mainly come from the solar neutrino experiments and the medium-baseline reactor experiment at KamLAND. A combined fit of Δm^2_{21} from the solar data once yields a small tension against the KamLAND reactor neutrino data under the assumption of the CPT conservation. This tension can be alleviated by the presence of a super-light sterile neutrino [1]. Due to the tiny mass splitting between the active and sterile neutrinos, the level-crossing and non-adiabatic transitions have to be taken into account during the propagation of solar neutrinos, and may lead to a large modification to the solar neutrino survival probability. Also, if the mass splitting between the sterile and active neutrinos is sufficiently small, the coherence between different mass eigenstates plays an important role as solar neutrinos travel from the Sun to the Earth.

Formalism

We consider the presence of a super-light sterile neutrino ν_s in addition to the three active neutrinos. In the 3+1 framework, the Hamiltonian of solar neutrinos becomes

$$H_f = U\mathrm{diag}(\frac{\Delta m^2_{01}}{2E_\nu}, 0, \frac{\Delta m^2_{21}}{2E_\nu}, \frac{\Delta m^2_{31}}{2E_\nu})U^\dagger + V\,, \tag{1}$$

where E_ν is the solar neutrino energy, Δm^2_{ij} the mass-squared differences, and the potential

$$V = \sqrt{2}G_F\mathrm{diag}(0, N_e - N_n/2, -N_n/2, -N_n/2)\,. \tag{2}$$

We parameterize the mixing matrix as $U \equiv \mathrm{diag}(1, U^{3\nu}) \cdot U_S$, where $U^{3\nu}$ is the standard three-neutrino mixing matrix, and the sterile mixing matrix is written as $U_S = R_{01}(\theta_{01}, \delta_{01}) \cdot R_{02}(\theta_{02}, \delta_{02}) \cdot R_{03}(\theta_{03}, \delta_{03})$. In general, the survival probability of solar neutrinos observed on the Earth can be written as

$$P_{ee} = \left|\sum_{i=0}^{3} U_{ei}e^{-i\frac{\Delta m^2_{i1}}{2E_\nu}L_0}A_{ei}\right|^2, \tag{3}$$

where L_0 is the distance between the Earth and the Sun. A_{ei} denotes the amplitude of the $\nu_e \to \nu_i$ transition inside the Sun, and can be written as

$$A_{ei} = \sum_{\alpha=s,e,\mu,\tau} U^\dagger_{i\alpha}\psi^{\rm SS}_{e\alpha}\,. \tag{4}$$

where $\psi^{\rm SS}_{e\alpha}$ is the amplitude of flavor transition $\nu_e \to \nu_\alpha$ from the center of the Sun to the surface of the Sun, and can be obtained by solving an 8-dimensional ODE with a numerical library from GSL. In Fig. 1, we show the survival probabilities in the 3+1 framework calculated with the numerical method for different values of $R_\Delta \equiv \Delta m^2_{01}/\Delta m^2_{21}$.

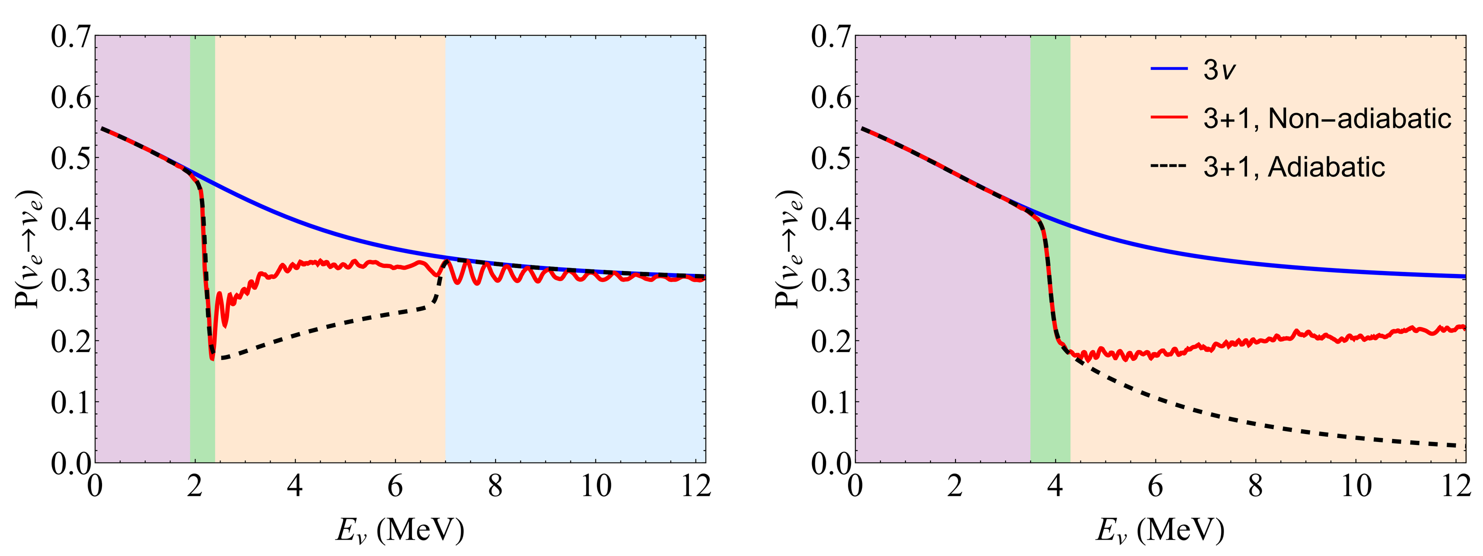

Figure 1. Survival probabilities of solar neutrinos as a function of neutrino energy for $R_\Delta = 0.15$ (left) and 1.20 (right).

Level crossing

We introduce λ_i to represent the first three eigenvalues of the Hamiltonian for convenience. Also, we take $\lambda_2 > \lambda_0 > \lambda_1$ ($\lambda_0 > \lambda_2 > \lambda_1$) for the case $R_\Delta < 1$ ($R_\Delta > 1$). The dependence of λ_i on the propagation distance inside the Sun is shown in Fig. 2. The left panel: (a) $R_\Delta = 0.15$, E_ν = 0.5 MeV; The middle panel: (b) $R_\Delta = 0.15$, E_ν = 10 MeV; The right panel: (c) $R_\Delta = 1.20$, E_ν = 10 MeV. The mixing angle θ_{01} is fixed to be $\sin^2 2\theta_{01} = 5 \times 10^{-4}$. The active-sterile resonance energy E_s can be determined by the resonance condition $\lambda_0 = \lambda_1$ or $\lambda_0 = \lambda_2$.

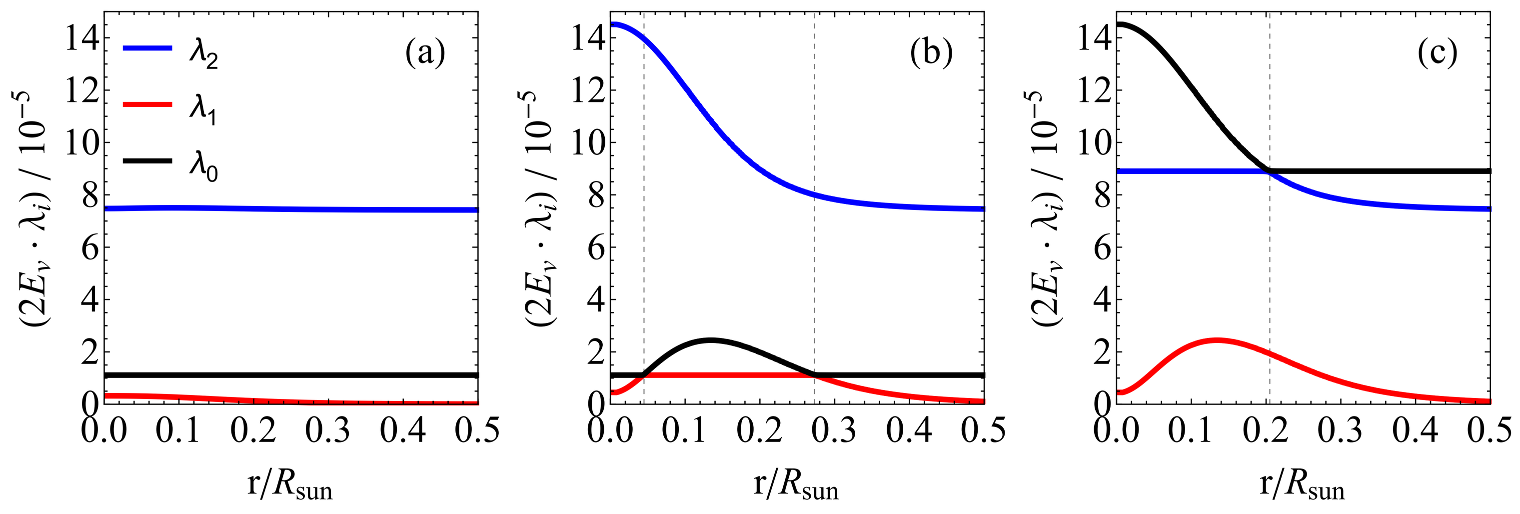

Figure 2. Three eigenvalues as a function of the propagation distance in the Sun.

Non-adiabatic effects

At low energies, we have $P_{ee} \approx P^{3\nu}_{ee} - |U_{e1}|^2 \left|U^{M_0}_{e0}\right|^2$. When E_ν becomes slightly larger than the first resonance energy E_{s1}, $\theta^{M_0}_{01}$ approaches $\frac{\pi}{2}$ in the center of the Sun, which will trigger a dip in P_{ee}. As E_ν increases, we have to take the non-adiabatic transition $\nu^M_0 \leftrightarrow \nu^M_1$ into account, and the presence of a nonzero phase between the transition amplitudes will cause small wiggles in P_{ee}. For $R_\Delta < 1$, ν_e produced in the center of the Sun basically consists of ν^M_2, and the non-adiabatic transition $\nu^M_0 \leftrightarrow \nu^M_1$ hardly has a impact on the survival probability, which yields P_{ee} approaches $P^{3\nu}_{ee}$ at high energies. For $R_\Delta > 1$, ν_e produced in the center of the Sun basically consists of $\nu^{M_0}_0$, which still causes a large discrepancy in P_{ee} at high energies. To illustrate the non-adiabatic effects, we plot $\left|U^{M_0}_{e0}\right|^2$ and P_{ee} for different values of R_Δ. The results are shown in the left and right panels of Fig. 3 for $R_\Delta < 1$ and $R_\Delta > 1$, respectively.

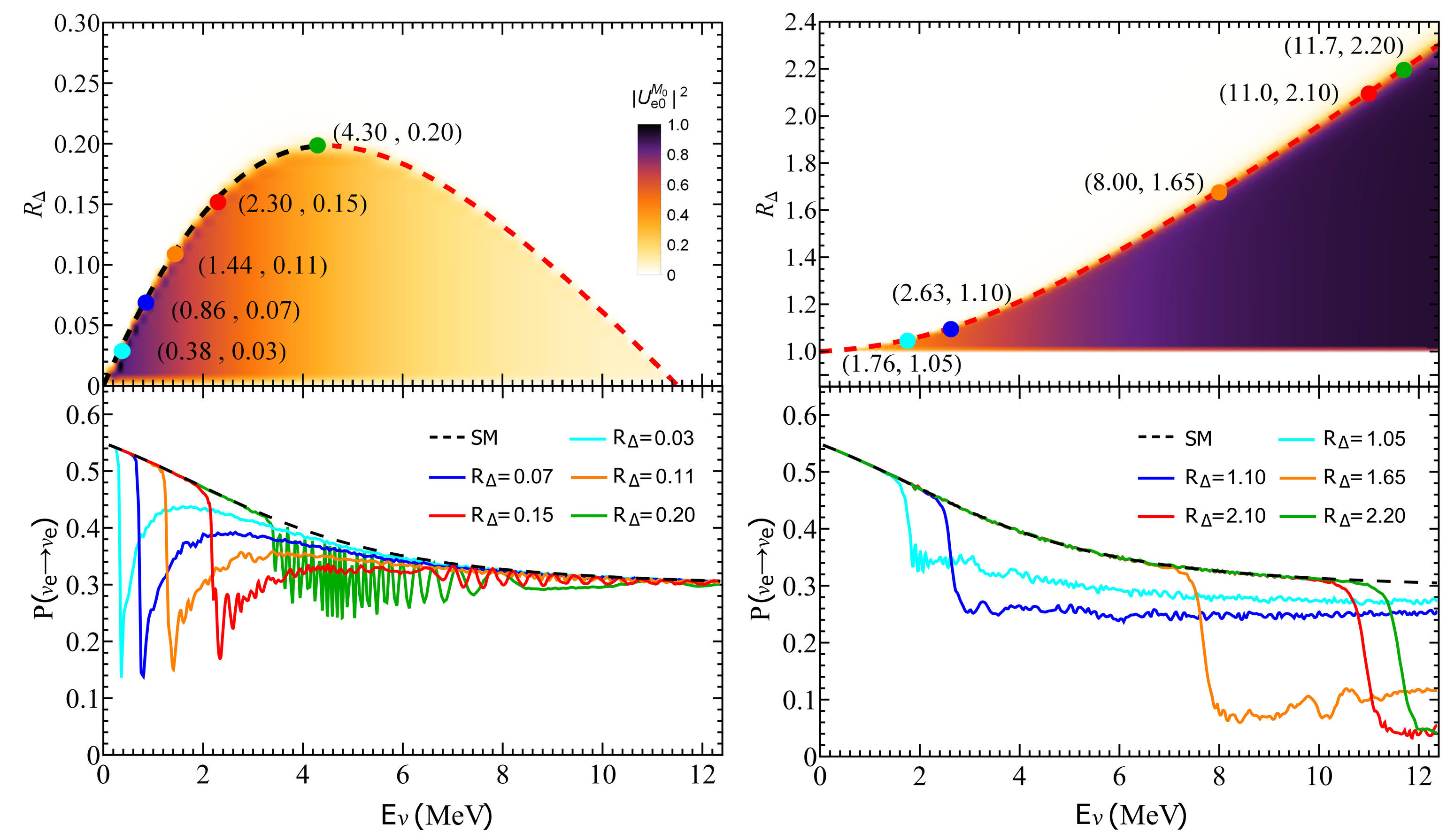

Figure 3. Upper panels: $\left|U^M_{e0}\right|^2$ as a function of neutrino energy and R_Δ. Lower panels: The survival probability as a function of neutrino energy for different values of R_Δ.

Constraints

Here we show the constraints on the sterile neutrino parameter space using current experimental data from Borexino and KamLAND for the case with only θ_{01} being nonzero as an example. The 95% CL bounds on $\sin^2 2\theta_{01}$ and Δm^2_{01} are shown in Fig. 4. In particular, we also present the separate bounds from the low and high energy solar neutrino data for comparison.

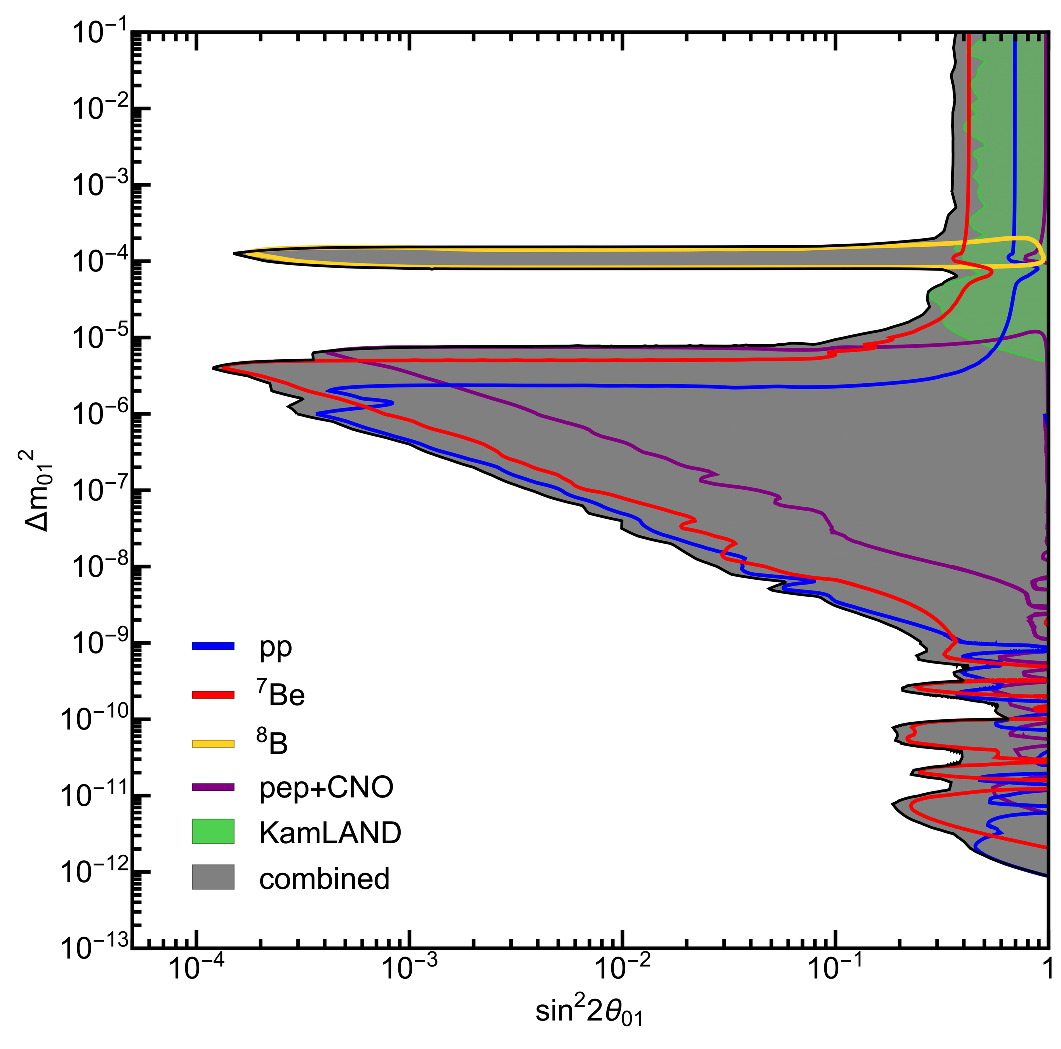

Figure 4. The 95 % CL bounds in the $(\sin^2 2\theta_{01}, \Delta m^2_{01})$ plane.

Conclusions

We find that the low and high energy solar neutrino data at Borexino are sensitive to different regions in the sterile neutrino parameter space. For the case with only θ_{01} being nonzero, the ^{8}B data sets the strongest bounds at $\Delta m^2_{01} \approx (1.1 \sim 2.2)\Delta m^2_{21}$, while the low energy solar neutrino data is more sensitive to other mass-squared regions. The lowest bounds on Δm^2_{01} from the pp data can reach 10^{-12} eV^2 because of the coherence effect. Also, due to the presence of non-adiabatic transitions, the bounds in the range of 10^{-9} eV$^2 \lesssim \Delta m^2_{01} \lesssim 10^{-5}$ eV^2 become weaker as Δm^2_{01} or $\sin^2 2\theta_{01}$ decreases. We also find that in the case with only θ_{02} or θ_{03} being nonzero, the low energy solar neutrino data set similar but weaker bounds as compared to the case with only θ_{01} being nonzero, but the bounds from the high energy solar data and the KamLAND data are largely affected by the nonzero mixing angles.

References

[1] P. C. de Holanda and A. Yu. Smirnov.
Solar neutrino spectrum, sterile neutrinos and additional radiation in the Universe.
Phys. Rev. D, 83:113011, 2011.